

Escape dynamics of photoexcited electrons at catechol:TiO₂(110)

L. Gundlach,* R. Ernstorfer, and F. Willig†

Dynamics of Interfacial Reactions, Hahn-Meitner-Institute Berlin, Glienicker Straße 100, 14109 Berlin, Germany

(Received 16 February 2006; revised manuscript received 18 May 2006; published 19 July 2006)

Ultrafast electron escape dynamics following excitation of the interfacial charge transfer complex of catechol prepared on the rutile TiO₂(110) surface was investigated with femtosecond two-photon photoemission (2PPE). Laser pulses were generated with two noncollinear optical parametric amplifiers operated simultaneously at a repetition rate of 150 kHz delivering a cross-correlation function with 35 fs full width at half maximum. Catechol was absorbed from the solution. The experimental data were not depending on the choice between three different solvents. Photoinduced interfacial charge transfer was instantaneous and thus the rise of the signal was controlled by the cross-correlation function. The energy distribution of the hot electrons generated at the surface was measured as 2PPE spectrum. The decay of the 2PPE signal was nonexponential with a first time constant below 10 fs, a dip in the 50 fs to 100 fs range, and a tail lasting for picoseconds. It was attributed to the release of the electrons from the surface and their escape into the bulk of the semiconductor.

DOI: 10.1103/PhysRevB.74.035324

PACS number(s): 73.20.-r, 78.47.+p, 79.60.Jv

I. INTRODUCTION

Light-driven interfacial electron transfer from a molecule to a solid is the primary event of many photoprocesses. Important examples can be found in photocatalytic reactions,^{1,2} in photovoltaic systems,^{3,4} and in the postulated field of molecular electronics.^{5,6} Time-resolved two-photon photoemission (TR-2PPE) is the method of choice for investigating ultrafast photodriven interfacial processes, provided the respective interface can be exposed to ultrahigh vacuum (UHV). As TR-2PPE is essentially an electron counting method, a high repetition rate laser system is desired. The TR-2PPE measurement collects simultaneously information on the energy distribution and the time evolution of the photogenerated electrons at the interface.^{7,8} The method offers far higher sensitivity than, e.g., transient absorption spectroscopy, since the photoemitted electrons can be collected directly by the detector. The 2PPE method can address a low density of photogenerated electrons and thus also a low coverage of molecules on the surface of a single crystal.^{9,10} TR-2PPE has frequently been used for analyzing electron dynamics at metal surfaces, in particular the dynamics of image potential states, adatoms, and small molecules.^{11–13} Work on semiconductor surfaces has mainly concentrated on silicon^{14,15} and on hot electron dynamics at the surface of III-V semiconductors.^{16,17}

We report here on the time-dependent escape of photo-generated electrons from the surface into the bulk of rutile TiO₂(110). The latter process was measured as time-dependent decay of 2PPE signals. For studying the escape of injected electrons from the surface into the bulk it is an obvious advantage if one can generate the electrons instantaneously in an optical transition on the surface of the semiconductor. This can be achieved in a direct optical charge transfer (CT) transition that lifts the electrons from the highest occupied molecular orbit (HOMO) of adsorbed catechol molecules to unoccupied electronic states of TiO₂. The closely related optical CT transition for a molecular complex comprising of three catechol molecules and one Ti atom has been known for quite some time.¹⁸ Electron injection

has been studied already with catechol adsorbed to nano-structured TiO₂ films.^{19–21} Subpicosecond mid-IR and visible transient absorption spectra on colloidal TiO₂ films with adsorbed catechol have confirmed that the electrons arrive on the Ti(3*d*) states of TiO₂ within the available time resolution, i.e., 100 fs in these experiments.²¹

A nanostructured TiO₂ film functions as an electron acceptor in dye-sensitized solar cells where the quantum yield for electron injection is close to one and the solar conversion efficiency at one sun can reach 10%.^{22,23} The direct optical charge transfer transition in the case of adsorbed catechol is an exception. For most of the other adsorbed dyes the distance between the chromophore and semiconductor is controlled by a larger anchor group and thus there is a finite time required for transferring the electron from the photoexcited chromophore to the surface of TiO₂. The corresponding injection times have been measured now from several ps down to the range of 10 fs applying transient absorption techniques.^{24–26} However, the escape of the electrons from the surface into the bulk of the semiconductor cannot be time resolved with the latter measuring technique. Therefore, the escape process is addressed here with TR-2PPE on the surface of a rutile single crystal with adsorbed catechol molecules to facilitate instantaneous optical generation of the electrons on the crystal surface.

Preparation and atomic structure of the bare (110) surface of rutile TiO₂ has been studied extensively over the last years (for a review, see Ref. 27). For the present work catechol was adsorbed on the clean (110) surface of rutile TiO₂ from solution. Adsorption from solution was preferred over evaporating catechol in UHV for two reasons. First, for carrying out the earlier measurements on catechol:TiO₂ systems the latter had been prepared and measured in different liquid environments.^{19–21} Second, adsorption from the solution at room temperature is the more powerful technique compared to evaporation since it also allows for adsorbing more complex molecules, e.g., aromatic chromophores, via anchor groups, such as carboxylic and phosphonic acid, that cannot be evaporated without suffering decomposition. Adsorption from the solution was carried out in a type of UHV chamber

specifically designed for this purpose. The important point here is to verify that the behavior of the adsorbate layer is not affected by the choice of the specific solvent. This is achieved most directly by measuring the adsorbate system after preparing it with different solvents.

The adsorption sites of catechol on the (101) surface of anatase TiO_2 have been studied theoretically by Redfern *et al.*²⁸ The results of these authors when applied to the (110) surface of rutile TiO_2 suggest that catechol forms a bidentate dissociative bridge-type site on the regular (110) rutile surface with each of the two O atoms of catechol forming a bond to two adjacent Ti atoms on the surface of TiO_2 . The adsorption of catechol onto the already cleaned rutile surface was carried out in a dedicated UHV chamber²⁹ that was specifically designed for preparation procedures where the bare cleaned surface of the semiconductor is the starting point. At UHV conditions, a small amount of degassed solution is brought into this UHV chamber after flooding it with ultra-pure argon, the solution is removed again, and the sample surface with the adsorbed molecules is then pumped down again to UHV conditions. Preparation, surface science characterization, sample transfer between the different UHV chambers, and TR-2PPE measurements always involved four different UHV chambers. One of these was a small mobile unit, equipped with a battery driven pump, for shuttling the sample between the other UHV chambers that were all equipped with load-lock ports. To ensure the reliability of this preparation procedure the sample was prepared using three different solvents and it was verified that the respective stationary and time-resolved electron spectra of the adsorbate system were reproduced and did not depend on properties of the specific solvent used in the preparation of the chosen adsorption layer. Since TR-2PPE is a pump-probe technique two ultrashort light pulses were necessary. The photon energy of the pump pulse (440 nm central wavelength) was in the absorption range of the direct optical charge transfer transition but was far too small for pumping a higher lying excited state of catechol or a band to band transition in TiO_2 . Pump and probe pulses (latter at 280 nm central wavelength) were generated by frequency doubling the outputs of two noncollinear optical parametric amplifiers (NOPA) resulting in a cross-correlation (CC) function of 35 fs width [fullwidth at half maximum (FWHM)] at 150 kHz repetition rate. With the absorption of the probe pulse hot electrons were photo-emitted from the surface of TiO_2 thereby generating the 2PPE signal. It was checked that the return of the injected electrons to the ionized catechol molecules lasted longer than the measured decay of the 2PPE signals. Thus, the recombination process did not control the decay of the 2PPE signal. Recombination, i.e., repopulation of the ground state, is difficult to measure with TR-2PPE. Therefore, the transient ground-state bleach was measured in UHV with catechol adsorbed to colloidal anatase TiO_2 films. Extensive investigations in our group of these systems, i.e., nanostructured anatase and rutile films and rutile $\text{TiO}_2(110)$ single crystals with the same adsorbed molecules, have revealed very similar time constants for corresponding electron transfer processes. Thus, the recombination time measured by transient absorption on the colloidal system in UHV can be taken as a measure of the recombination time in the catechol: TiO_2 rutile system.

The shape of the ultraviolet photoemission spectroscopy (UPS) and 2PPE spectra for catechol adsorbed on $\text{TiO}_2(110)$ is controlled by the same reorganization energy and by the same Franck-Condon factors as the optical CT transition. It is well known that reorganization energy and Franck-Condon factors have a decisive influence on the shape of a CT absorption spectrum.^{30,31}

The dynamics of electron escape from the surface, as measured here for instantaneous electron injection with catechol, does not depend on the specific nature of the organic molecule. Replacing catechol by another organic molecule, e.g., perylene attached via a carbonic acid group as anchor,²⁴ adds a finite electron transfer time for bringing the electron from the excited molecular donor state to the surface of TiO_2 (Refs. 32 and 33) but the escape dynamics remains unchanged as measured with catechol.³³

We report here on the escape dynamics measured with TR-2PPE representing the case of instantaneous optical generation of electrons on the surface of rutile TiO_2 . The escape dynamics for the electrons from the surface of TiO_2 with the ionized catechol molecules into the bulk of TiO_2 was found nonexponential with an initial decay time below 10 fs, followed by a time constant in the range of 100 fs, and a final decay lasting to several picoseconds. The escape process has been simulated in theoretical models for a time window shorter than 100 fs by Rego and Batista³⁴ and most recently for a time window of several 100 fs by Duncan *et al.*³⁵ The measured decay reported in the present paper agrees well with the time scale predicted by the theoretical papers.

II. EXPERIMENT

The femtosecond laser system was based on a commercial amplified 150 kHz Ti:sapphire oscillator operating at 800 nm which pumped two NOPAs. The NOPA principle,³⁶ commonly used for 1 kHz systems, was adapted to a high repetition rate by our group in cooperation with the group of Prof. Riedle.²⁵ Tunable sub-20 fs pulses in the visible and 15 fs pulses from second harmonic generation (SHG) of a near infrared (NIR) output pulse were generated with the first NOPA. This setup required 90% of the Ti:sapphire output power, such that the remaining 10% could in principle be used to generate the UV pulse that is necessary for TR-2PPE by third harmonic generation (THG). However, due to the limited acceptance bandwidth of nonlinear crystals THG leads to fairly long pulses which would thus restrict the temporal resolution of the experiment. To obtain shorter pulses, the remaining 10 percent of the fundamental output was used instead to generate a white light continuum in a sapphire plate. The 400 nm beam at the exit of the first NOPA was employed again to amplify a broad spectral slice of the above continuum seed in a second NOPA setup. The whole experimental procedure has been described in detail in Ref. 13. The visible output of this second NOPA was frequency doubled in a 75 μm thick beta-barium borate (BBO) crystal to obtain a spectrally broad UV pulse centered at 280 nm. As the 400 nm pump pulse had a reduced power at the exit of the first NOPA and since its mode was slightly distorted due to the first conversion process, the second NOPA yielded less

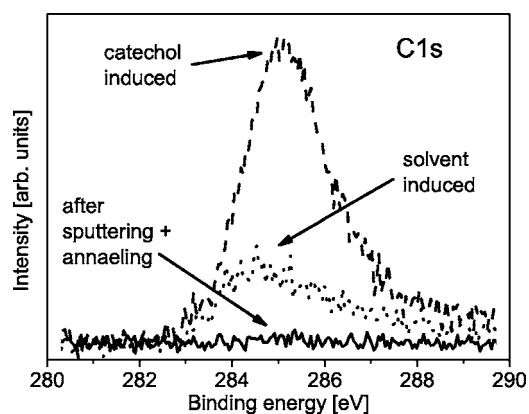


FIG. 1. XPS spectra of C 1s on TiO₂ samples: after four sputtering-annealing cycles as described in the text (straight line), after immersing the cleaned TiO₂ sample in pure CCl₂H₂ solvent (dotted line), and after adsorption of catechol from CCl₂H₂ solution (dashed line).

pulse energy than the first. But spectral width and compressibility were comparable to the output of the first NOPA. Pulse compression was achieved with standard fused silica prism compressors prior to carrying out the SHG processing.³⁷

Four separate UHV chambers were used for preparing, characterizing, and finally measuring a sample with 2PPE or transient absorption. All chambers had a base pressure in the range below 5×10^{-10} mbar. Two of the UHV chambers were tightly screwed to the surface of the laser table and were floating with it. They consisted of subchambers such that preparation steps and actual time-resolved measurements could be carried out in subchambers separated by valves. The third UHV chamber was equipped with instrumentation for low-energy electron diffraction (LEED), UPS, and x-ray photoemission spectroscopy (XPS) for characterizing the samples. The fourth UHV chamber was a small mobile unit, equipped with a battery powered ion getter pump, serving as a shuttle for the samples between the other UHV chambers. All the chambers were equipped with load-lock ports facilitating sample transfer under UHV conditions. One of the UHV chambers was specifically designed for adsorbing molecules from solution on the surface of a solid.²⁹ The corresponding preparation procedure is outlined below.

Many details of the experimental equipment used here for preparing and characterizing the molecule: semiconductor interface have been described before in conjunction with a patented contamination-free metal-organic chemical-vapor deposition-UHV sample transfer system.³⁸ The XPS spectrum of every commercial rutile crystal (Crystal GmbH, Berlin) showed a pronounced carbon peak that was ascribed to organic impurities. In the next step the (110) surface of the rutile crystal was cleaned and ordered by carrying out repeated cycles of Ar⁺ ion bombardment (700 eV, 3 μ A, 10 min) and heating (875 K, 10 min) similar to recipes given in the literature.³⁹ At the same time the C 1s peak in the XPS spectra disappeared (Fig. 1) and the well-known clear 1×1 LEED image⁴⁰ appeared. In addition Fig. 1 shows the C 1s peak after adsorption of catechol from methylene chloride solution (dashed line) and the C 1s peak measured on a

cleaned TiO₂ sample that was exposed to pure methylene chloride under the same UHV conditions as described for the catechol preparation. It should be noted that the amount of residual carbon from the solvent is expected to be even less on the catechol coated surface since catechol is known to replace other adsorbates, i.e., methanol.⁴¹ No chemical shift for the C 1s peak was observed between the samples prepared with three different solvents. The thus prepared sample showed sufficient conductivity for carrying out photoelectron spectroscopy. The conductivity is mainly due to Ti interstitials.^{42,43} The Fermi level of the thus treated sample was found just below the conduction band edge.

The adsorption procedure started with the already cleaned and ordered rutile crystal mounted at the tip of the sample holder and suspended above the opening of a cuvette mounted below in the UHV chamber. At this stage the chamber was at a base pressure below 5×10^{-10} mbar. In the next step it was flooded with ultrapure argon. A small amount of the solvent containing the catechol molecules had been filled already into a small glass flask that was protected by a closed valve from laboratory air and was connected through a valve and a stainless steel pipe to the UHV chamber. Prior to introducing the solvent containing 0.1 mM catechol molecules into the glass flask this part of the set up had been pumped down to 1×10^{-3} mbar, heated with a hot-air gun, and then filled with ultrapure argon prior to introducing a small aliquot of the solvent with the dye molecules. The latter was a degassed dye solution handled with the well-known Schlenk technique up to introducing it through the valve into the glass flask connected to the UHV system.

To ensure that the measured electron spectra, in particular the TR-2PPE spectra, are reproducible and independent of the solvent used to prepare the sample the adsorption layer was prepared with three different solvents and the behavior of the systems was compared. First, a mixture of 75% dried toluene and 25% dried methanol was used to enable the comparison with earlier measurements carried out for the adsorption of other dyes from the same solvent in our group. Second, pure toluene was used to check in specifically on the possible influence of methanol. And third, methylene chloride was used since the latter allows one to check via XPS for residual solvent on the prepared surface.

About 40 ml of the dye solution was sucked into the cuvette inside the UHV chamber by driving it through the stainless steel pipes with a small pressure gradient. For the next preparation step the rutile crystal was lowered into the cuvette and, after a typical contact time of 20 min, it was removed again from the cuvette. The interface with the thus adsorbed catechol molecules was rinsed several times following the above procedure but only with the pure solvent to remove any catechol not bonded to the surface. Finally, the last solvent was sucked out of the UHV chamber and the latter pumped down again to 5×10^{-10} mbar. It is reasonable to expect as the result of the above adsorption procedure a complete coverage of the available adsorption sites with catechol. For comparison 2PPE measurements were carried out not only on the above interface with the adsorption layer but also on rutile crystals that were prepared with the identical preparation procedure but where only the solvent was used in the absence of catechol. The latter samples gave much

smaller 2PPE signals for identical pump and probe pulses and showed a distinctly different time dependence.

A few remarks appear in order here concerning the possible role of the solvent molecules. Adsorption of only methanol molecules on the surface of rutile has been studied by Henderson *et al.*⁴⁴ These authors have reported that the majority of the methanol molecules adsorb without dissociating and desorb from the surface already at 295 K. Methanol was found to adsorb dissociatively at fivefold coordinated Ti atoms from where the fragments desorbed at 350 K. Methanol was also found to desorb dissociatively at oxygen vacancies from where the fragments desorbed at 480 K.⁴⁴ The samples investigated here reached about 360 K while they were illuminated with a halogen lamp during sample alignment. According to the results of Henderson *et al.* only methanol that was adsorbed at vacancy sites could have survived on the surface prepared as described above. The corresponding defect concentration has been reported in the range of 8% for samples heated prior to methanol adsorption to 850 K in vacuum,⁴⁴ as was the case for our samples. Whereas for toluene no data are available to our knowledge, temperature programmed desorption (TPD) for the closely related benzene adsorbed on TiO₂(110) have shown molecular desorption at 260 K.⁴⁵ Wong *et al.*⁴⁶ and Lu *et al.*⁴⁷ have reported on TPD measurements of chloroform adsorbed on TiO₂(110). Chloroform desorbed molecularly between 150 and 200 K.

Since the chemical shift in XPS for the C 1s peak is expected to be small between toluene and catechol, the absence of residual solvent molecules after preparation was confirmed by preparing a sample with methylene chloride as solvent. On this sample no contribution of chlorine to the measured XPS spectrum could be detected after preparation. From the different XPS measurements on the differently prepared samples we conclude that recontamination of the samples due to the preparation procedure with the solvents is negligible. In addition all three samples showed nearly identical transient signals in TR-2PPE.

For interpreting the time dependence of the 2PPE signals it was important to check on the recombination time in the catechol:TiO₂ system, i.e., the time scale for the return of the injected electron to the hole left behind on the ionized catechol molecule. Since the latter cannot be measured easily with a 2PPE signal a different approach was taken. Detailed investigations in our group of nanostructured anatase and rutile films and of TiO₂(110) single crystals with the same adsorbed molecules have revealed very similar time constants for corresponding electron transfer processes.^{32,33} Accordingly, the recombination time measured by transient absorption on the colloidal system in UHV can be considered also as the recombination time in the catechol:TiO₂ rutile system measured in UHV.

To obtain the transient absorption data colloidal TiO₂ films were prepared with a thickness of about 1 μm on 45 μm glass where the recipe followed the procedure described by Nazeeruddin *et al.*²² Prior to adsorbing catechol on the anatase film the latter was heated at 450 °C for 45 min in air. Catechol was adsorbed onto the colloids from the same solution that was used in the case of the rutile single crystals. The dye-covered nanostructured TiO₂ film

was rinsed several times with the solvent, dried under argon, and quickly transferred to the UHV chamber designed for carrying out transient absorption measurements. The same 440 nm pump pulse was used as for TR-2PPE, but the second NOPA was tuned in this case to 480 nm since the probe pulse had to address ground-state absorption of adsorbed catechol. The cross correlation for the transient absorption measurements was measured on a SiC diode with 45 fs width (FWHM).

III. RESULTS AND DISCUSSION

The positions of the electronic levels for the adsorbed molecule relative to those for the semiconductor have a great influence on the photoinduced interfacial charge transfer dynamics.⁴⁸ The HOMO for catechol adsorbed on the rutile surface can be estimated from ultraviolet photoemission spectroscopy (UPS). One has to keep in mind that, as known from gas phase UPS of molecules, the electron spectrum includes a vibrational structure. This structure evolves when a molecule initially in its vibrational ground state is left in a higher vibrational state after the electron is emitted. Energy conservation demands that the kinetic energy of the emitted electron is reduced by the amount of energy that is converted into vibrational energy of the molecule after ionization. Another consequence is that the intensity of the different vibrational transitions is controlled by the Franck-Condon overlap of the initial molecular state with the ionized molecular state. Thus, the 0,0 transition, i.e., the electronic transition where the molecule stays in its vibrational ground state, is located on the low binding-energy side of a molecular peak in UPS, since in this case all the photon energy is converted into kinetic energy of the electron.

Assuming that an inhomogeneous broadening not larger than 250 meV reveals the true vibrational width of the spectrum with the peak leading to the maximum at 1 eV above the valence band edge in the UPS measurement shown in Fig. 2 (dashed line), the position of the HOMO (0,0 transition) can be estimated at about 1 eV below the Fermi level and thus 2 eV above the valence band edge. The position of the HOMO is indicated in Fig. 2 by a vertical line. Thus upon adsorption on the (110) surface of rutile TiO₂ the ionization potential (IP) of catechol⁴⁹ is shifted to lower energy by about 2.5 eV against the value for catechol in the gas phase. Such shifts of the IP are also reported for other adsorbate:substrate systems and are ascribed to the wave function mixing between substrate and adsorbate.⁵⁰

In addition Fig. 2 shows two photoemission spectra, one for occupied ground states of the bare TiO₂ surface (UPS measurements, dotted curves) and the other for the population in unoccupied states that was generated due to excitation of the catechol CT complex by the pump pulse of the laser (2PPE spectrum, solid curve). In the latter case, the pump pulse (440 nm, 2.8 eV) lifted an electron from the occupied HOMO of adsorbed catechol molecules to empty Ti(3d) states localized on the surface of TiO₂. Comparable to the case of direct photoionization in the UPS measurement, discussed above, the catechol molecule can gain vibrational energy during the CT transition. As a result, the electron is

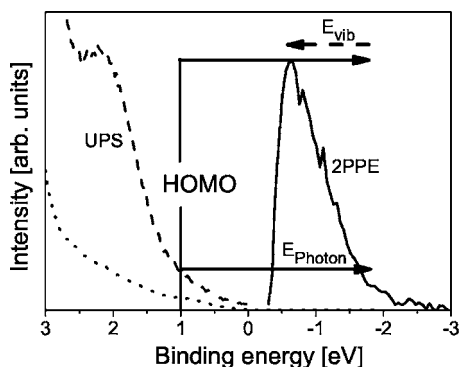


FIG. 2. UPS and 2PPE spectra of catechol adsorbed on $\text{TiO}_2(110)$. The 2PPE spectrum is shown vs the energy of the corresponding intermediate states. Zero energy corresponds to the position of the Fermi level in the system. The dotted UPS spectrum is that of $\text{TiO}_2(110)$ in the absence of catechol. The estimated energy of the HOMO level of adsorbed catechol is indicated by the vertical line labeled HOMO. The two horizontal arrows indicate the photon energy of the pump pulse. The 0,0 transition of the optical charge transfer (CT) transition leads to the unoccupied electronic state at the tip of the horizontal arrow. The dashed arrow in the opposite direction on top of the upper solid arrow indicates the vibrational excitation energy generated in the ionized catechol product state of the optical CT transition that corresponds to the maximum Franck-Condon factor. Further details are explained in the text.

injected into TiO_2 acceptor states with a higher binding energy. The second pulse promoted the electron further to electronic levels above the vacuum energy where it could reach the time of flight (TOF) detector. The kinetic energy of the electrons was determined from the time of flight inside the drift tube of the detector. By adding the difference in the work functions of the sample and TOF and subtracting the photon energy of the probe pulse, the intermediate state energy was obtained with respect to the conduction band edge. As usual the work function of the sample was determined for every sample from the secondary electron edge in the 2PPE spectrum (not shown).

The energy distribution of the 2PPE spectrum was simply identified here with that in the intermediate states by subtracting the energy of the second photon. If we assume that the intermediate states are bulk states the correction for the density of states in bulk rutile TiO_2 (Ref. 51) would not change the distribution significantly. However, the intermediate states may be at least partially of a different nature, as will be discussed below. The UPS spectrum of the bare TiO_2 surface is shown for comparison as the dotted curve. The dashed UPS spectrum was measured for the catechol: $\text{TiO}_2(110)$ system.

Adding the photon energy of the pump pulse to the HOMO energy (horizontal arrows in Fig. 2) leads to the electronic intermediate state with the highest energy since in this case there is no vibrational excitation of the ionized catechol product state in the optical CT transition. The corresponding optical CT transition corresponds to the 0,0 optical transition for the photon energy of the pump pulse. It should be noted that each of the many electronic levels with different energies on the surface of the semiconductor can give

rise to such a 0,0 CT transition from the HOMO of adsorbed catechol when the appropriate photon energy is supplied. This distinguishes a CT transition at a surface complex from the optical excitation of a CT transition in a molecular complex.

In general vibrational excitation of the ionized catechol product state will consume, however, part of the energy supplied by the fixed photon energy of the pump pulse. In the latter case the corresponding electronic acceptor level will have a correspondingly lower energy than that of the 0,0 transition. This partitioning of the fixed photon energy between the energy of the electronic product state on the surface of TiO_2 and the vibrational excitation energy deposited in the ionized catechol is illustrated in Fig. 2 by the solid horizontal arrow and by the dashed arrow on top pointing in the opposite direction. The electron population generated in the respective unoccupied electronic level is controlled by the respective Franck-Condon factor. The dashed arrow labeled E_{vib} in Fig. 2 is pointing to the electronic level with the maximum intermediate state electron population corresponding to the maximum Franck-Condon factor of the optical CT transition. Of course, the actual population generated in the respective electronic level is also influenced by the energy-dependent density of unoccupied electronic states at the interface and by the transition probability for photoemission from the respective electronic intermediate state into vacuum. The latter two effects can modify the actual intermediate state population with respect to the measured kinetic energy distribution in the 2PPE spectrum but the qualitative conclusions will remain unaltered. Both the spectra in Fig. 2, i.e., UPS and 2PPE, suggest that the reorganization energy, i.e., the difference between the energy of the 0,0 transition and that with the maximum Franck-Condon factor, is in the range of 0.5–1 eV. A more precise value for the reorganization energy would require the detailed knowledge of first the energy-dependent density of electronic acceptor states at the interface and second the probability for photoemission from the respective intermediate state. The above value for the reorganization energy does not appear unusual for a CT transition involving the ionization of a fairly small molecule like catechol.³⁰ From the optical CT transition of the molecular complex of three catechol units with one Ti atom, e.g., from Fig. 4 in Ref. 18, one can deduce directly a reorganization energy on the order of 0.9 eV.

The adsorption configuration of catechol on anatase $\text{TiO}_2(101)$ has been discussed by Persson *et al.*⁵² based on semiempirical calculations. More recently, the same system was calculated by Redfern *et al.*²⁸ based on semiempirical as well as density functional theory (DFT) calculations. Persson *et al.* have suggested a dissociative adsorption, i.e., removal of the two H atoms, which is bidentate and bridge type, i.e., where the bonds are formed by the two oxygen atoms to two different Ti atoms on the surface. Redfern *et al.* have discussed several adsorption configurations in more detail and have considered also relaxation of the surface atoms. Their data show that a dissociative bidentate configuration with the two oxygen atoms of catechol forming bonds to just one Ti atom requires a specific defect site. The latter is formed on the surface of very small anatase clusters (diameter smaller than 2 nm) but not on larger clusters or on the planar (101)

surface of an anatase single crystal. The authors also conclude that the above bridge-type bidentate dissociative configuration is competing with monodentate and nondissociative configurations, i.e., molecular adsorption retaining the two -OH groups, on the latter surfaces. Since the distance between adjacent Ti atoms on the (110) surface of rutile can accommodate bidentate bridge-type bonds to catechol with a smaller lattice relaxation than is required on the (101) surface of anatase, we adopt here the arguments of Redfern *et al.* also for the rutile (110) surface. The large shift by close to 2.5 eV of the catechol HOMO upon adsorption on TiO₂ (compare above) and the red edge of the CT transition at 620 nm suggest that the dissociative bridge-type bidentate configuration is the dominant adsorption configuration on the rutile surface. A few remarks appear in order regarding the optical CT transition. Our measurements of the CT absorption (not shown here) in the case of catechol adsorbed to large diameter (50 nm) rutile colloids and on large (20 nm) anatase colloids coincide from 620 nm up to 400 nm, and they agree perfectly with the data of Wang *et al.*⁵³ except for the expected earlier rise due to the band-band transition in the case of rutile which is known to have a smaller band gap than anatase. It should be noted that the CT absorption curves for catechol adsorbed on crystalline rutile or anatase do not show the pronounced maximum that is seen in the CT absorption of molecular compounds formed by three catechol units and only one Ti atom.¹⁸ In the case of catechol adsorbed to crystalline TiO₂ there is a continuum of electronic 0,0 transitions, each leading from the HOMO of catechol to an unoccupied electronic level on the surface of TiO₂, as discussed above. Thus, one can picture the CT absorption for the latter system as a superposition of many spectra with a shape seen for the molecular compound of catechol with only one Ti atom.¹⁸ Since Franck-Condon factors for the case of a large reorganization energy are controlling the shape of the CT spectrum^{30,31} one has to compare the red edge of the experimental CT absorption spectrum with the energy of the calculated CT transition as has been correctly identified by Redfern *et al.*²⁸ As a corollary the electronic CT transition recently calculated by Duncan *et al.* for the molecular catechol-Ti compound⁵⁴ is in even better agreement with the experimental data^{18,53} than has been realized in the respective paper.

The absorption depth of 300 nm light in TiO₂ is 90 nm,⁵⁵ the escape depth for the excited electrons is not exactly known. The “universal curve” for the inelastic mean free path does not reflect the escape depth for electrons with a very low kinetic energy since elastic scattering has to be taken into account.⁵⁶ However, the upper limit according to the universal curve is 90 nm at 1 eV kinetic energy.⁵⁷ The actual value will be significantly smaller. For example, calculations on SiO₂ where elastic scattering has been taken into account have predicted an escape depth of 10–15 Å for kinetic energies between 1 and 10 eV.⁵⁶ Comparable values have been predicted for GaAs.⁵⁸ Thus, the population of electrons generated in the unoccupied electronic states was probed by the 2PPE signal in a very narrow spatial range near the surface of the order of 15 Å width. In order to judge on the measured time behavior of the electron population generated in the unoccupied electronic states it is important

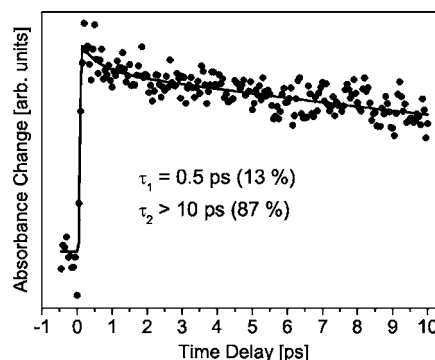


FIG. 3. Transient bleach of catechol ground state measured at 480 nm after 440 nm excitation (dots). Biexponential fit of the data with the printed parameters.

to know on what time scale the electron will return to the ionized catechol left behind on the surface and recombine there to form again the ground-state catechol. The electrons will eventually undergo this latter recombination reaction since there is no other effective sink competing in the present system for the electrons. The system will deliver of course a photocurrent if a closed circuit is formed as is the case in a dye-sensitized electrochemical cell. The time scale of the above recombination reaction was determined from the time-dependent disappearance of the ground-state bleach signal. It was measured as a transient absorption signal with 440 nm pump and 480 nm probe pulses in a colloidal TiO₂ system sensitized with catechol and measured in a UHV chamber as described above. Transient absorption was chosen for this measurement since 2PPE measurements are not very suitable for measuring ground state bleach and recovery. There have been reports already of such a measurement by Wang *et al.* who carried out transient absorption spectroscopy in a similar system in solution.⁵³ They have found that the transient spectra of catechol on TiO₂ colloids do not show any significant spectral shift. An isosbestic point at 510 nm separates the ground-state bleach ranging from 420 to 510 nm from the transient absorption of the injected electrons. The reported bleach recovery kinetics is multiexponential with 62% of a 0.4 ps component, 19% of a 8 ps component, and longer components. Figure 3 shows the bleach recovery kinetics measured by transient absorption spectroscopy in UHV together with the biexponential fit curve. Most of the signal recovered within >10 ps. The fast recombination rate with 0.5 ps time constant can be attributed to electrons trapped in shallow traps in the vicinity of the ionized catechol molecules. Whereas the time constants measured here are comparable to the ones reported earlier by Wang *et al.*,⁵³ the amplitude ratios are different. This difference may be due to the difference in the environment, i.e., UHV against laboratory air, or to a slightly different preparation of the colloids. Nevertheless, both the transient absorption measurements show that the early time-dependent disappearance of the 2PPE signal of the electrons generated in the unoccupied states is much faster than recombination and thus the measured early time decay is not dominated by the latter process.

Energy distributions were measured at different delay times between pump and probe pulse. As the energy of the

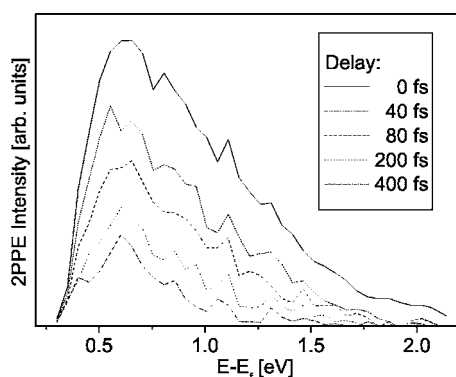


FIG. 4. 2PPE spectra for the catechol coated rutile TiO_2 surface at different time delays.

pump pulse was smaller than the band gap of TiO_2 , the bare surface of rutile contributed just a weak 2PPE signal originating from defect-induced occupied gap states. The corresponding 2PPE background signal covered a wide energy range with the same time dependence as the CC, thus indicating a very fast decay. The energy of the probe pulse was close to the work function of the sample. The corresponding one-photon photoemission signal was subtracted from the 2PPE signal. Figure 4 shows 2PPE energy distributions measured at different time delays. The spectra show a continuous distribution over an energy range covering 1 eV with a maximum value at 0.6 eV and a long tail to higher energies. The contributions above 1.7 eV decay very fast and are attributed to the bulk background signal of the sample. The exact position of time zero (t_0) and the pulse width were extracted at 2 eV kinetic energy. At this energy the time trace gave the identical CC of both pulses as found on a $\text{Cu}(111)$ single crystal. Width and shape of the spectrum with a peak at 0.6 eV are very similar to the ground-state photoionization spectrum measured by UPS. As explained in connection with Fig. 2 the shape of the 2PPE spectra is controlled to a large degree by the reorganization energy and the Franck-Condon factors of the optical CT transition whose 0,0 energy corresponds to the high-energy onset of the spectrum. The shape of the spectrum can be modified to some degree by an energy-dependent density of unoccupied electronic states at the surface of the catechol:rutile (110) interface and also by an energy-dependent photoemission probability from these intermediate states. The peak position at about 0.6 eV is consistent with the measured peak position of the molecular HOMO 2 eV above the valence band edge when one takes into account the 2.8 eV photon energy of the pump pulse and the reorganization energy of around 1 eV that leads to a corresponding shift of the peak position to lower energies from the energy of the 0,0 transition at the maximum kinetic energy (see discussion of Fig. 2).

The electronic acceptor states at the catechol:rutile (110) interface are not known. They are expected to comprise unoccupied surface resonances and bulk states reaching to the interface. Detailed DFT calculations of the electronic states at a reconstructed $\text{InP}(100)$ surface with the dangling bonds saturated by P-H bonds show for example a lower density of surface resonances close to the band edge and an increas-

ingly higher density to higher energies.⁵⁹ The surface resonances become the more bulklike the higher their energy. The measured 2PPE spectra (Fig. 4) show a continuous distribution of collected electrons over an energy range wider than 1 eV.

Recently, our group has investigated the influence of a specific surface resonance on time dependent 2PPE spectra for In-rich reconstructed $\text{InP}(100)$, both experimentally and theoretically.⁶⁰ Both the time dependence and the continuous energy distribution in the spectra shown in Fig. 4 do not show any sign of a single dominant surface resonance for the catechol:rutile (110) interface prepared as described above. Thus, we expect only minor modifications from an energy-dependent variation in the density of states. This is expected for the known bulk density of states for bare rutile (110) in this energy range.⁵¹ In cooperation with a theory group we have investigated recently the influence of specific final and intermediate states on the shape of 2PPE spectra.^{60,61} In the case of InP it was found that the experimental data are much less influenced by a mismatch in the effective mass of intermediate and final state than would be expected for the free electron as the final state. Since this is an unexplored area and since the shape of Fig. 4 is as expected and similar to the optical CT spectrum of the catechol:Ti complex, we conclude that the measured kinetic energy spectrum (2PPE) in Fig. 4 is mainly controlled by the reorganization energy and the Franck-Condon factors of the optical CT transition with the 0,0 energy in the range of 1.5 eV (compare Fig. 2). The Franck-Condon factors dictate the energy distribution and electron population in the intermediate electronic states of the 2PPE signal.

Figure 4 shows an additional rather surprising result, i.e., the energy distribution is hardly changing with increasing delay time, a behavior that is strikingly different from, for example, the hot electron relaxation in the case of $\text{InP}(100)$ that has been measured also with 2PPE.^{60,62} The surprising conclusion here is that the energy relaxation of the electrons injected into the unoccupied states at the catechol:rutile (110) interface is negligible on the time scale of the measured decay, i.e., 200 fs. The same observation has been made for electron injection into rutile (110) from the excited state of various perylene dyes.³³ It should be noted in Fig. 4 that there is neither an obvious shift in the peak position nor in other features of the spectrum with increasing time delay. Even at a delay time of 300 fs neither the peak position nor the shape of the spectrum have changed to any significant extent.

A possible explanation for this unusual behavior may be the difference in the charge separation process in both these cases. The TR-2PPE measurement of InP involved a band-band transition where the electron as well as the hole are delocalized in the bulk bands and are virtually not interacting with each other due to the actual screening. The measurements of the catechol: TiO_2 interface presented here involved an electron transfer process, where the acceptor states are believed to differ from bulk states due to contributions from unoccupied surface resonances and/or adsorbate-induced interface states. Furthermore, in the latter case the hole stays localized on the catechol molecule and the amount of screening is not known. Thus, the behavior of the electrons gener-

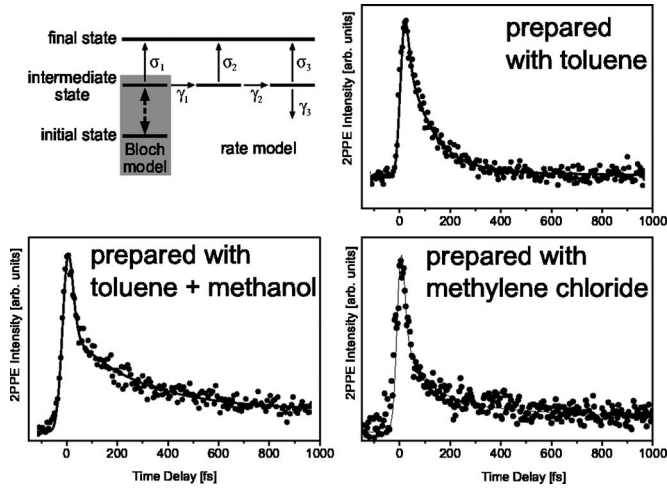


FIG. 5. Time traces at 600 meV intermediate state energy (circles) and fitted curves using the model shown in the inset (lines) for three catechol adsorption layers prepared with three different solvents as indicated. Fit parameters are shown in Table I.

ated at the catechol:TiO₂ interface is attributed to these electronic states with virtually no dispersion, and only very slow energy exchange between these different states. Furthermore, bulk band-structure calculations reveal a high effective mass already for bulk electrons at the Γ point^{63,64} which are expected to be even more localized at the surface.

The escape of the electron from the surface was measured by the TR-2PPE signal at 0.6 eV intermediate state energy. Figure 5 shows the time trace for samples prepared with different solvents. All transients show a very rapid initial decay and a long-lived background. The amount of this long-lived background is different for the different samples. One possible reason for this difference may be a different coverage with catechol molecules. The solvent molecules may block efficiently possible binding sites for catechol as long as the TiO₂ sample is in contact with the solution. Thus, the surface coverage with catechol may depend on the strength of the interaction between the solvent and the surface of TiO₂. For example, the probe pulse is absorbed by catechol and this decreases the slow decay component where the electrons have reached a larger distance.

Another possibility may be a small amount of residual solvent molecules on the surface after the sample was brought back to UHV conditions. Such residual solvent molecules may result in additional trap states for the injected electrons. Both mechanisms discussed above are possible explanations for the larger, long-lived background signal measured on the sample prepared with the addition of methanol in the solvent. However, a more detailed analysis by means of optical Bloch equations and rate equations is given in the following text and shows that this subtle difference does not affect the results drawn from the measurements. Fit curve and the underlying fit model are shown in Fig. 5. The photoemission step was taken into account by convoluting the intermediate state population with the probe pulse.⁶⁸ The temporal shift of the peak against t_0 , the rise, and also the very early decay of the signal were all fitted by means of optical Bloch equations for a two-level system representing

TABLE I. Fit parameter for the Bloch plus rate constant model depicted in Fig. 5 for the samples prepared with three different solvents.

Solvent	τ_1 (fs)	τ_2 (fs)	τ_3 (fs)	σ_1	σ_2	σ_3
Toluene	2	97	804	1	0.08	0.004
Toluene+methanol	2	85	945	1	0.04	0.01
Methylene chloride	2	93	1366	1	0.04	0.01

the initial ground and the intermediate excited state. This model is analogous to the one discussed in detail in Ref. 65. This model predicts a monoexponential decay. As the measured decay was nonexponential, however, this simple model could not fit the measured decay at longer times. Therefore, the Bloch model was combined with a two-level rate model (inset of Fig. 5). The latter was appropriate since it turned out that the coherence decayed very fast (<10 fs). Photoionization can be described classically for times where the coherence has decayed prior to the arrival of the probe pulse.⁶⁶ The contributions of the consecutive spatial positions in the escape process to the 2PPE signal were weighted by σ_i factors, thereby modeling Lambert-Beer's law and also the escape depth of photoelectrons. Thus, the parameters γ_i and σ_i model the escape of electrons and the detection probability, respectively, in a phenomenological way. The time constants ($\tau_i = \frac{1}{\gamma_i}$) resulting from the fit model depicted in Fig. 5 for the catechol adsorption layers prepared with three different solvents are shown in Table I.

The deviation of the time constants between the differently prepared samples is of the same order of magnitude as the reproducibility of the measurements.³³ Obviously, influences of the solvent on the surface, especially on the acceptor states for the optical CT transition, are negligible. The latter are controlled by the formation of the catechol:Ti bonds if they are specific surface resonances.

Since energy relaxation was negligible in the observed 2PPE signals the decay must be ascribed to the escape of the electrons from the detection depth of 2PPE. The measured time decay (Fig. 5) with the strongest dip in the time scale of 50 to 100 fs can be understood from a crude estimate. With the escape depth for the 2PPE signal in the range of 5 to 15 Å (compare above) the above time scale would imply an electron mobility on the order of 10 cm² V⁻¹ s⁻¹. This estimate follows from the well-known Einstein relationship between diffusion coefficient and mobility together with the well-known relationship between distance and time scale for diffusion. Room temperature electron mobilities referring to the band edge are 1.4 cm² V⁻¹ s⁻¹ and 8 cm² V⁻¹ s⁻¹ for directions perpendicular and parallel to the c axis, respectively.⁶⁷ Since screening of the injected electrons via relaxation of the nuclei in the oxide lattice is not expected to be complete within 50 fs one can expect a higher effective mobility for the escape process of the hot electrons than corresponds to the electron mobility at the band edge. Moreover, one can expect that the Coulombic attraction between the positive charge left behind on the catechol molecule and the electron generated on the surface of TiO₂ must play a role

for the escape process. Thus, simple model considerations as presented above are certainly not sufficient. Fortunately, there are recent *ab initio* calculations of the time-dependent escape of the electrons available for closely related systems. Rego and Batista have carried out combined DFT and quantum dynamical calculations on this system to investigate the interfacial electron transfer dynamics.³⁴ A cluster of TiO₂ with adsorbed catechol was treated instead of the catechol:(110) TiO₂ interface. These authors have reported that the injected electron is initially localized on the Ti⁴⁺ surface ions next to the catechol followed by an anisotropic escape of the electron.⁶⁹ The escape times vary by up to one order of magnitude for different crystallographic directions. The above model calculations covered only an initial time window of 20 fs. Most recently, Duncan *et al.* have calculated the escape of electrons from alizarin on the surface of a TiO₂ slab over a longer time span of several 100 fs with nonadiabatic molecular dynamics simulations.³⁵ The system is closely related to the experimental system investigated in this work. The escape from near-surface states to bulklike states was found nonexponential with a dominant time constant of 100 fs.³⁵

Our experimental data shown in Fig. 5 are obviously in qualitative agreement with the latter model calculations. Fur-

ther 2PPE experiments carried out with other organic chromophores adsorbed to the (110) surface of rutile TiO₂ will be described elsewhere. The latter data show the same escape dynamics (Fig. 5) as reported here for the case of adsorbed catechol.

IV. CONCLUSIONS

Ultrafast dynamics of electron escape from the surface into the bulk of rutile (110) TiO₂ was measured with 2PPE following optical excitation of the charge transfer transition in the catechol:Ti surface complex. The decay of the 2PPE signal started with a time constant below 10 fs, showed a dominant dip in the range of 50 fs to 100 fs and lasted with a tail up to picoseconds. The measured escape behavior for the injected electrons is in fair qualitative agreement with the first *ab initio* calculations of Rego and Batista and Duncan *et al.* for the corresponding escape process.

ACKNOWLEDGMENT

L.G. (SPP 1093) and R.E. (SFB 450) thank the German Science Foundation for financial support.

*Electronic address: gundlach@hmi.de

†Electronic address: willig@hmi.de

¹J. W. Gadzuk, Phys. Rev. Lett. **76**, 4234 (1996).

²C. P. Koch, T. Klüner, and H.-J. Freund, J. Chem. Phys. **119**, 1750 (2003).

³B. O'Regan and M. Grätzel, Nature (London) **353**, 737 (1991).

⁴C. Brabec, G. Zerza, N. Sariciftci, G. Cerullo, G. Lanzani, S. D. Silvestri, and J. Hummelen, in *Ultrafast Phenomena XII: Proceedings of the 12th International Conference, Charleston*, edited by T. Elsaesser, S. Mukamel, M. M. Murnane, and N. F. Scherer, Springer Series in Chemical Physics Vol. 66 (Springer, Berlin, 2000), pp. 589–592.

⁵*Molecular Electronics*, edited by M. Ratner and J. Jortner (Blackwells, Oxford, 1997).

⁶J. Heath and M. Ratner, Phys. Today **56** (5), 43 (2003).

⁷R. Haight, Surf. Sci. Rep. **21**, 275 (1995).

⁸H. Petek and S. Ogawa, Prog. Surf. Sci. **65**, 239 (1997).

⁹W. Zhao, W. Wei, and J. M. White, Surf. Sci. **547**, 374 (2003).

¹⁰Q. Zhong, C. Gahl, and M. Wolf, Surf. Sci. **496**, 21 (2002).

¹¹K. Boger, M. Weinelt, and T. Fauster, Phys. Rev. Lett. **92**, 126803 (2004).

¹²I. L. Shumay, U. Höfer, C. Reuß, U. Thomann, W. Wallauer, and T. Fauster, Phys. Rev. B **58**, 13974 (1998).

¹³L. Gundlach, R. Ernstorfer, E. Riedle, R. Eichberger, and F. Willig, Appl. Phys. B **80**, 727 (2005).

¹⁴T. Sjödin, H. Petek, and H.-L. Dai, Phys. Rev. Lett. **81**, 5664 (1998).

¹⁵M. Weinelt, M. Kutschera, T. Fauster, and M. Rohlfing, Phys. Rev. Lett. **92**, 126801 (2004).

¹⁶L. Töben, L. Gundlach, T. Hannappel, R. Ernstorfer, R. Eichberger, and F. Willig, Appl. Phys. A **78**, 239 (2004).

¹⁷L. Töben *et al.*, Phys. Rev. Lett. **94**, 067601 (2005).

¹⁸B. A. Borgias, S. R. Cooper, Y. B. Koh, and K. N. Raymond, Inorg. Chem. **23**, 1009 (1984).

¹⁹J. Moser, S. PUNCHIHEWA, P. P. Infelta, and M. Grätzel, Langmuir **7**, 3012 (1991).

²⁰Y. Liu, J. I. Dadap, D. Zimdars, and K. B. Eisenthal, J. Phys. Chem. B **103**, 2480 (1999).

²¹E. Hao, N. A. Anderson, J. B. Asbury, and T. Lian, J. Phys. Chem. B **106**, 10191 (2002).

²²M. K. Nazeeruddin, A. Kay, I. Rodicio, R. Humphry-Baker, E. Müller, P. Liska, N. Vlachopoulos, and M. Grätzel, J. Am. Chem. Soc. **115**, 6382 (1993).

²³N.-G. Park, G. Schlichthörl, J. van de Lagemaat, H. M. Cheong, A. Mascarenhas, and A. J. Frank, J. Phys. Chem. B **103**, 3308 (1999).

²⁴B. Burfeindt, T. Hannappel, W. Storck, and F. Willig, J. Phys. Chem. **100**, 16463 (1996).

²⁵R. Ernstorfer, L. Gundlach, C. Zimmermann, F. Willig, R. Eichberger, and E. Riedle, in *Ultrafast Optics IV: Selected Contributions to the 4th International Conference on Ultrafast Optics*, F. Krausz, G. Korn, P. Corkum, and I. A. Walmsley, eds., Springer Series in Optical Sciences, Vol. 95 (Springer, Berlin, 2004), pp. 393–398.

²⁶R. Huber, J.-E. Moser, M. Grätzel, and J. Wachtveitl, J. Phys. Chem. B **106**, 6494 (2002).

²⁷U. Diebold, Surf. Sci. Rep. **48**, 53 (2003).

²⁸P. C. Redfern, P. Zapol, L. A. Curtiss, T. Rajh, and M. C. Thurnauer, J. Phys. Chem. B **107**, 11419 (2003).

²⁹R. Ernstorfer, F. Willig, T. Hannappel, and S. Kubala, Deutsches Patentamt, patent pending.

³⁰N. S. Hush, Prog. Inorg. Chem. **8**, 391 (1967).

- ³¹K. Huang and A. Rhys, Proc. R. Soc. London, Ser. A **204**, 406 (1950).
- ³²R. Ernstorfer, Ph.D. thesis, Freien Universität Berlin, 2004.
- ³³L. Gundlach, Ph.D. thesis, Freien Universität Berlin, 2005.
- ³⁴L. G. C. Rego and V. S. Batista, J. Am. Chem. Soc. **125**, 7989 (2003).
- ³⁵W. R. Duncan, W. M. Stier, and O. V. Prezhdo, J. Am. Chem. Soc. **127**, 7941 (2005).
- ³⁶E. Riedle, M. Beutter, S. Lochbrunner, J. Piel, S. Schenkl, S. Spörlein, and W. Zinth, Appl. Phys. B **71**, 457 (2000).
- ³⁷I. Z. Kozma, P. Baum, S. Lochbrunner, and E. Riedle, Opt. Express **11**, 3110 (2003).
- ³⁸T. Hannappel, S. Visbeck, L. Töben, and F. Willig, Rev. Sci. Instrum. **75**, 1297 (2004).
- ³⁹M. Li, W. Hebenstreit, L. Gross, U. Diebold, M. A. Henderson, D. R. Jennison, P. A. Schultz, and M. P. Sears, Surf. Sci. **437**, 173 (1999).
- ⁴⁰S. Reiß, H. Krumm, A. Niklewski, V. Staemmler, and C. Wöll, J. Chem. Phys. **116**, 7704 (2002).
- ⁴¹M. Lorenzi, Master's thesis, EPF Lausanne, No. 2389, 2001.
- ⁴²M. A. Henderson, W. S. Epling, C. L. Perkins, and C. H. F. Peden, J. Phys. Chem. B **103**, 5328 (1999).
- ⁴³M. A. Henderson, Surf. Sci. **419**, 174 (1999).
- ⁴⁴M. A. Henderson, S. Otero-Tapia, and M. E. Castro, Faraday Discuss. **114**, 313 (1999).
- ⁴⁵S. Suzuki, Y. Yamaguchi, H. Onishi, T. Sasaki, K.-I. Fukui, and Y. Iwasawa, J. Chem. Soc., Faraday Trans. **94**, 161 (1998).
- ⁴⁶J. C. S. Wong, A. Linsebigler, G. Lu, J. Fan, and John T. Yates, Jr., J. Phys. Chem. **99**, 335 (1995).
- ⁴⁷G. Lu, A. Linsebigler, and John T. Yates, Jr., J. Phys. Chem. **99**, 7626 (1995).
- ⁴⁸S. Ramakrishna, F. Willig, V. May, and A. Knorr, J. Phys. Chem. B **107**, 607 (2003).
- ⁴⁹M. H. Palmer, W. Moyes, M. Speirs, and J. N. A. Ridyard, J. Mol. Struct. **52**, 293 (1979).
- ⁵⁰T. Vondrak and X.-Y. Zhu, J. Phys. Chem. B **103**, 3449 (1999).
- ⁵¹K. M. Glassford and J. R. Chelikowsky, Phys. Rev. B **45**, 3874 (1992).
- ⁵²P. Persson, R. Bergström, and S. Lunell, J. Phys. Chem. B **104**, 10348 (2000).
- ⁵³Y. Wang, K. Hang, N. A. Anderson, and T. Lian, J. Phys. Chem. B **107**, 9434 (2003).
- ⁵⁴W. R. Duncan and O. V. Prezhdo, J. Phys. Chem. B **109**, 365 (2005).
- ⁵⁵SOPRA-NK database, URL: <http://www.sopra-sa.com/more/database.asp>
- ⁵⁶H.-J. Fitting, E. Schreiber, Kuhr, and A. von Czarnowski, J. Electron Spectrosc. Relat. Phenom. **119**, 35 (2001).
- ⁵⁷R. Brundle, J. Vac. Sci. Technol. **11**, 212 (1974).
- ⁵⁸I. Bartoš and W. Schattke, Surf. Rev. Lett. **6**, 631 (1999).
- ⁵⁹P. H. Hahn and W. G. Schmidt, Surf. Rev. Lett. **10**, 163 (2003).
- ⁶⁰L. Töben *et al.*, Phys. Rev. Lett. **94**, 067601 (2005).
- ⁶¹S. Ramakrishna, F. Willig, and A. Knorr, Surf. Sci. **558**, 159 (2004).
- ⁶²L. Töben, Ph.D. thesis, Technische Universität Berlin, 2002.
- ⁶³M. Mikami, S. Nakamura, O. Kitao, H. Arakawa, and G. Gonze, Jpn. J. Appl. Phys., Part 2 **39**, L847 (2000).
- ⁶⁴S. Munnix and M. Schmeits, Phys. Rev. B **30**, 2202 (1984).
- ⁶⁵T. Hertel, E. Knoesel, M. Wolf, and G. Ertl, Phys. Rev. Lett. **76**, 535 (1996).
- ⁶⁶C. Timm and K. H. Bennemann, J. Phys.: Condens. Matter **16**, 661 (2004).
- ⁶⁷E. Hendry, F. Wang, J. Shan, T. F. Heinz, and M. Bonn, Phys. Rev. B **69**, 081101(R) (2004).
- ⁶⁸The autocorrelation of the probe pulse was measured prior to the experiment on a Cu(111) sample.
- ⁶⁹In the calculations of Rego and Batista (Ref. 34) electron transfer was assumed to start from the excited lowest unoccupied molecular orbital state of catechol.